19e Journées de l'Hydrodynamique
26 – 28 novembre 2024, Nantes

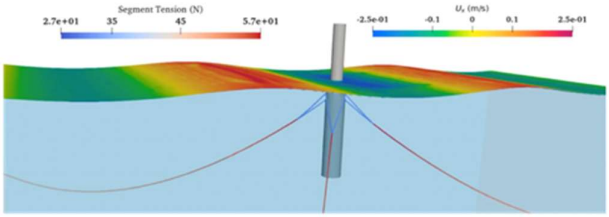

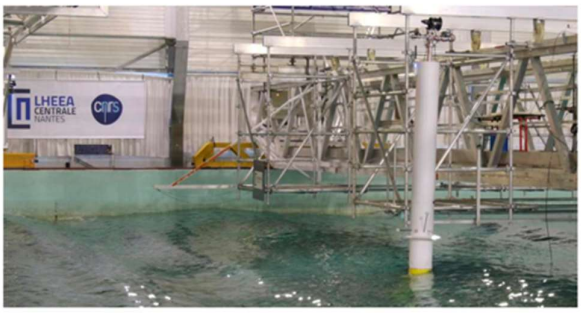

ETUDE EXPERIMENTALE ET NUMERIQUE DES CUVES ANTI-ROULIS – COMPARAISONS AVEC ESSAIS EN BASSIN ET RETOUR D'EXPERIENCE

NUMERICAL AND EXPERIMENTAL STUDY OF ANTI-ROLL TANKS – COMPARISONS WITH BASIN TESTS AND RETURN OF EXPERIENCE

L. DIEBOLD[(1)], A. BLANC[(1)], G. DE-HAUTECLOCQUE[(1)]
louis.diebold@bureauveritas.com ; arthur.blanc@bureauveritas.com ;
guillaume.de-hauteclocque@bureauveritas.com

[(1)] Département Recherche, Division Marine & Offshore, Bureau Veritas, Paris La Défense

Résumé

Une méthodologie cohérente de prise en compte des cuves anti-roulis dans un code potentiel de tenue à la mer est présentée. Afin de valider cette méthodologie, différents types d'essais sont présentés. Tout d'abord, des essais de mouvements forcés sur une configuration typique de cuve anti-roulis sont présentés. Ces essais de mouvements forcés permettent de valider les calculs CFD pour l'évaluation de la réponse de ces cuves anti-roulis. Ensuite, la notion d'angle effectif de gravité (EGA) est présentée et validée. Cette quantité d'EGA est utilisée afin d'établir une méthodologie cohérente de prise en compte des cuves anti-roulis dans un code potentiel de tenue à la mer. Cette méthodologie est validée par comparaison avec des essais en bassin et des mesures au réel effectuées sur un porte-conteneurs instrumenté. Enfin, les coefficients de réduction de roulis typiques pour ce type de porte-conteneurs sont présentés.

Summary

A consistent methodology for considering anti-roll tanks in a potential seakeeping code is presented. To validate this methodology, different types of tests are presented. First, forced motion tests on a typical anti-roll tank configuration are presented. These forced motion tests allow the validation of CFD (Computational Fluid Dynamics) calculations for evaluating the response of these anti-roll tanks. Then, the notion of Effective Gravity Angle (EGA) is presented and validated. This EGA quantity is used to establish a consistent methodology for considering anti-roll tanks in a potential seakeeping code. This methodology is validated by comparison with basin tests and full-scale measurements carried out on an instrumented container ship. Finally, the typical roll reduction coefficients for this type of container ship are presented.

I – Introduction

The transportation of containers by sea is a crucial component of global trade and logistics. Container ships play a vital role in this supply chain, allowing for the efficient movement of goods around the world. The design of container ships must ensure the safety of transporting the loaded containers while enabling the optimization of loading capacities. In practice, containers on deck are secured by means of lashing bridges permanently connected by welding to the ship structure. These lashing bridges allow lashing at a higher level and so optimization of the cargo handling capacities. The capacity of these lashing bridges is ruled by the maximum roll acceleration that be encountered by the ship during its voyage. To mitigate these roll accelerations, devices such as bilge keels, stabilizer fins and anti-roll tanks (ARTs) may be installed. On actual container ships, bilge keels are already implemented and increasing their size or installing stabilizer fins would induce larger drag and so a (non-acceptable) decrease of the ship's speed. ARTs offer a solution to such a problem. Indeed, ARTs do not bring any additional drag. Only free surface ARTs are considered in this paper: U-tubes are not considered. Therefore, ARTs refer to free surface passive ARTs in the whole paper.

The objective of this paper is to present a consistent methodology for considering ARTs in a potential seakeeping code and to apply it to evaluate the roll reduction brought by these devices. To validate this methodology, different types of tests are presented. First, forced roll motion tests on a typical anti-roll tank configuration are presented. These forced motion tests allow the validation of CFD (Computational Fluid Dynamics) calculations for evaluating the response of these ARTs. Then, the notion of Effective Gravity Angle (EGA) is presented and validated. This EGA quantity is used to establish a consistent methodology for considering ARTs in a potential seakeeping code. This methodology is validated through comparison with basin model tests and full-scale measurements carried out on an instrumented container ship. Finally, the typical roll reduction coefficients for this type of container ship are presented.

II – Methodology for anti-roll tanks

II – 1 Overall methodology (NR 625 - Structural Rules for Container Ships, 2016)

As already mentioned above, the capacity of the lashing bridges is ruled by the maximum roll acceleration that be encountered by the ship during its voyage. For safety reasons, BV considers this maximum acceleration as being this one associated with a 25-year return period. By default (without any ART), this value can be easily calculated using a regression formula (BV NR625, Ch.4, Sec 2.1.1). This formula considers mainly the following parameters: the roll radius of gyration (kr), the metacentric height (GM) and the ship's breadth. By entering these values in the lashing software, the ship's captain ensures the safe loading of containers on board. In order to take into account the roll reduction brought by ARTs, the following roll reduction factor (defined below) is to be entered by the ship's captain:

$$f_{ART} = \frac{\theta_{ART}}{\theta_{wo-AR}} = \frac{Extreme\ Long\ Term\ Roll\ Angle\ with\ ART\ (25y - RP)}{Extreme\ Long\ Term\ Roll\ Angle\ without\ ART\ (25y - RP)} \quad (1)$$

Where:

- θ_{ART} : Direct calculation of the extreme long term roll angle (25-year return period for the North Atlantic scatter diagram) including the effect of the anti-roll tank (ART)
- θ_{wo-ART} : Direct calculation of the extreme long term roll angle (25-year return period for the North Atlantic scatter diagram) without the effect of the anti-roll tank (ART)

The objective of this paper is to propose a (validated) methodology to derive such roll reduction factors for a range of operational metacentric heights (typically, GM ranging from 1.5m to 15.0m).

II – 2 Reference frames and notations

In this section, we consider two different reference frames:

- $\{G_0, \vec{x}, \vec{y}, \vec{z}\}$ where G_0 denotes the center of gravity of the system {ship+ARTs} at rest, the x-axis point towards the ship bow, the y-axis points towards portside and the z-axis points upwards. This is an inertial reference frame.
- $\{C, \vec{x}', \vec{y}', \vec{z}'\}$ is the tank-fixed reference frame, where C denotes the ART center of volume. At rest, $(\vec{x}', \vec{y}', \vec{z}')$ corresponds to $(\vec{x}, \vec{y}, \vec{z})$. This reference frame is not an inertial one.

II – 3 Ship motions equation

Within the linear potential theory, the equation of motion of a ship equipped with ARTs can be expressed ((Malenica Š., 2003)) as follows in $\{G_0, \vec{x}, \vec{y}, \vec{z}\}$:

$$\left(-\omega^2\left(\left[M_{G_0}^{notk}\right] + \left[A_{G_0}\right]\right) - i\omega\left[B_{G_0}\right] + \left[C_{G_0}\right]\right)\left\{\xi_{G_0}\right\} = \left\{F_{G_0}^{DI}\right\} + \left\{F_{G_0}^{Liq}\right\} \quad (2)$$

where $\left\{\xi_{G_0}\right\}$, $\left[M_{G_0}^{notk}\right]$, $\left[A_{G_0}\right]$, $\left[B_{G_0}\right]$, $\left[C_{G_0}\right]$, $\left\{F_{G_0}^{DI}\right\}$ and $\left\{F_{G_0}^{Liq}\right\}$ denote respectively the rigid ship motions (6 d.o.f.), the ship inertia (where the equivalent ARTs solid inertia are subtracted), the added mass matrix, the damping matrix, the stiffness matrix, the forces and moments due to the incident and diffracted waves and the liquid forces due to the ARTs. All terms (except the liquid forces due to ARTs) are calculated using a potential code such as HydroSTAR© (see (Chen, 2004)).

The liquid forces due to the ARTs ($\left\{F_{G_0}^{Liq}\right\}$) are evaluated either by Computational Fluid Dynamic (CFD) calculations either by dedicated model tests.

II – 4 EGA definition

The Effective Gravity Angle (EGA) is defined in (Carette, 2015) as follows:

$$EGA(t) = \arctan\left(\frac{\ddot{y}(t)}{\ddot{z}(t)}\right) \quad (3)$$

where $\ddot{y}(t)$ and $\ddot{z}(t)$ are the ship-fixed (non-inertial reference frame) lateral and vertical accelerations, including gravity (directed upwards). More physics insight about the EGA and the demonstration that EGA is a governing parameter for ARTs response are given in the section III.3.

a) Pure roll motion

In case of pure roll motion $\phi(t)$, the ship-fixed transverse and vertical accelerations (including gravity directed upwards) are equal to $\ddot{y}(t) = g\sin(\phi(t))$ and $\ddot{z}(t) = g\cos(\phi(t))$ giving the following EGA:

$$EGA(t) = \arctan\left(\frac{g\sin(\phi(t))}{g\cos(\phi(t))}\right) = \phi(t) \quad (4)$$

So in case of pure roll motion, the EGA is equal to the roll motion.

b) Pure sway motion

In case of pure sway harmonic motion, the ship-fixed transverse and vertical accelerations (including gravity directed upwards) are equal to $\ddot{y}(t) = -\omega^2 y_0 \sin(\omega t)$ and $\ddot{z}(t) = g$, giving the following EGA:

$$EGA(t) = \arctan\left(\frac{-\omega^2 y_0 \sin(\omega t)}{g}\right) \underset{\text{lin.}}{\Rightarrow} EGA_a = \frac{-\omega^2 y_0}{g} \quad (5)$$

where EGA_a denotes the amplitude of the linearized EGA.

The above equation expresses a relation between the sway and EGA amplitudes.

II – 5 Relation between EGA and ship motions

As it will be shown in section III.3, EGA is a governing parameter for the ART response: the ART response can be expressed as a function of the EGA. To establish a consistent methodology for considering anti-roll tanks in a potential seakeeping code, one needs to express the EGA as function of ship motions. This is the objective of this section.

Thus, the ART response can be written as follows $\{F_C^{Liq}\}_{|C} = \{F_C^{ega}\}_{|C} EGA_C$ where $\{F_C^{ega}\}_{|C}$ and EGA_c denotes respectively the nondimensionalized ART response and the EGA at the ART center of volume (C). To express this ART response in terms of ship motions, the two following steps are considered.

First, EGA_c (EGA at the ART center of volume) can be expressed in terms of ship motions at the ship's center of gravity G_0 in the inertial reference frame. To do so, the accelerations at C are first transferred from the ship-fixed reference frame to the inertial one. Then, these accelerations are transferred (in the inertial reference frame) from the center of volume C to the ship's center of gravity G_0. Keeping only first order terms, one gets the following relation:

$$EGA_C \underbrace{=}_{lin} [B]\{\xi_{G_0}\} \tag{6a}$$

$$\text{with } [B] = \left[0 \quad \frac{-\omega^2}{g} \quad 0 \quad 1 + \frac{\omega^2 Z_C}{g} \quad 0 \quad \frac{-\omega^2 X_C}{g}\right] \tag{6b}$$

where X_C=x(C)-x(G_0), Y_C=y(C)-y(G_0) et Z_C=z(C)-z(G_0).

Second, the ART response $\{F_C^{ega}\}_{|C}$ is expressed at G_0 (ship's center of gravity).

With $\{F_C^{ega}\}_{|C} = (F_1 \quad \dots \quad F_6)$, we obtain the following relation:

$$\{F_C^{ega}\}_{|R} = [F]^T \tag{7a}$$

$$\text{with } [F] = [F_1, F_2, F_3, F_4 + Y_C F_3 - Z_C F_2, F_5 + Z_C F_1 - X_C F_3, F_6 + X_C F_2 - Y_C F_1] \tag{7b}$$

where $X_C = x(C) - x(G_0)$, $Y_C = y(C) - y(G_0)$ and $Z_C = z(C) - z(G_0)$.

Finally, one gets the following relation:

$$\{F_C^{Liq}\}_{|C} = ([F]^T . [B])\{\xi_{G_0}\} \tag{8}$$

II – 6 Iterative procedure to solve EGA problem – regular waves:

As previously mentioned, the ART response (calculated by CFD or measured during model tests) is non-linear so the solution of the coupled equation of motion (Eq.3) depends on the EGA amplitude of the forced motion for ART. To address this issue, one can apply an iterate procedure to get convergence on the EGA motion amplitude. In details, the final EGA at the center of volume of the ART is to be equal to the initial EGA considered to calculate the ART response. This iteration procedure is figured out below:

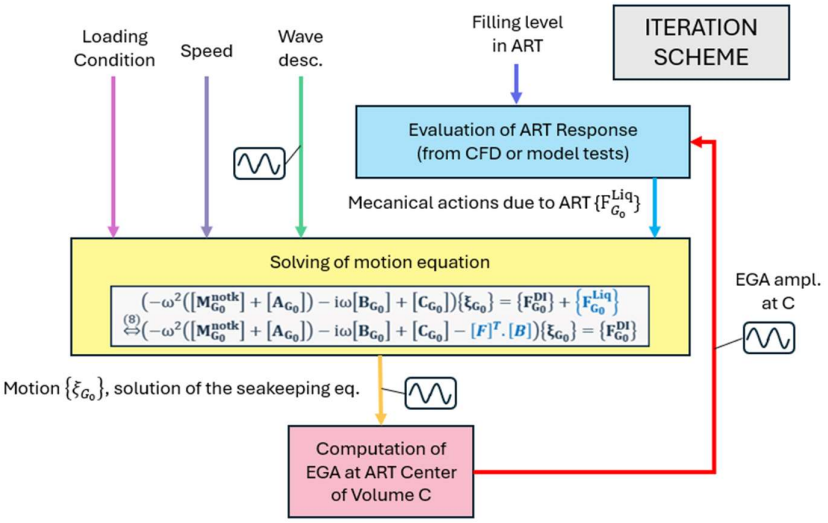

Figure 1a: Iterative procedure for the EGA, regular case.

II – 7 Iterative procedure to solve EGA problem – irregular sea-state:

The case of irregular waves is more complex and raises some questions. When the mechanical resolution considers not a single regular wave but the description of a sea-state as input, the output is a statistic on motions, and therefore on EGA. The described procedure to solve EGA problem implies a unique value of EGA amplitude to estimate the mechanical efforts due to the ART. The procedure needs to be adapted by adding an extra step to derive a metric of the amplitude of the EGA cycles from the output EGA distribution. The underlying assumption is that the additional roll damping provided by the tank on the sea state corresponds to the one provided by the tank assuming a unique EGA amplitude equal to this metric. To date, no mathematical justification has been established for defining this value. Based on the empirical observations, it is proposed to complete the procedure by applying the $EGA_{1/3}$ metric (average of the largest third of cycles). This metric qualitatively describes the amplitude of the large EGA cycles and in practice has produced motion statistics that are consistent with a few on-board measurements.

II – 8 Iterative procedure to solve EGA problem – roll damping linearization:

A key quantity when resolving the roll motion is roll damping. When evaluating the roll reduction due to the use of ART, it is essential to correctly evaluate the hydrodynamic contribution to roll damping. A commonly used description of roll damping is based on linear and quadratic roll coefficients. This description of damping requires linearization when solving the equation of motion. This linearization (harmonic in the case of a regular wave, stochastic in the case of a wave spectrum) allows an equivalent linear roll coefficient to be derived from the linear and quadratic damping coefficients and the standard deviation of the roll speed response. An additional loop on roll motion is then to be added to the procedure.

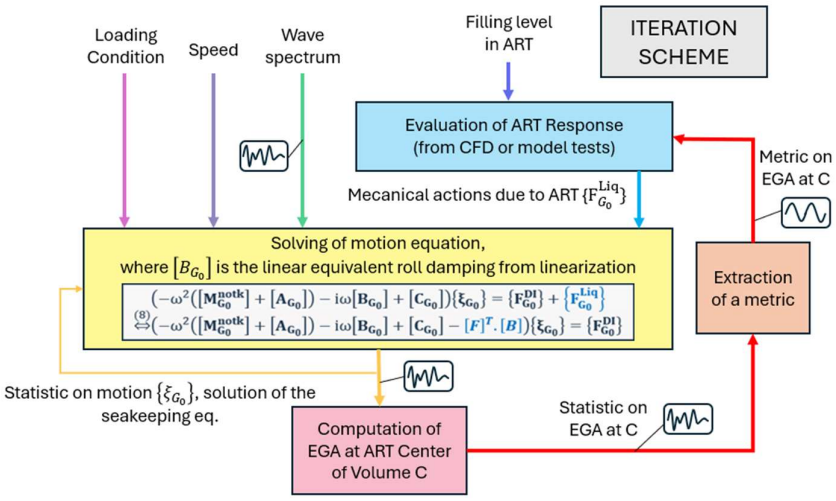

Figure 1b: Iterative procedure for the EGA, irregular case with damping linearization.

II – 9 Long-term calculations :

The procedure described above allows to calculate a roll response for a given short-term sailing condition (sea state and speed), a loading condition and a level of filing in ART. Following the discussion in II – 7. From an operational point of view, the quantity of interest is derived from long-term quantities. Therefore, a long-term statistic needs to be reconstructed from the set of loading conditions, operating conditions and sea states that the ship is likely to encounter during its operation. In practice, a scatter diagram is given, as well as an operational profile, so that we know the probability of any loading condition, filling level and sailing condition combination.

Then, following the procedure described in II - 7, a "short-term" EGA problem is solved for each of these configurations, and as many "short-term" distributions are derived.

Finally, the long-term roll statistic is reconstructed from the "short-term" distributions of each of the configurations, and their probability according to following relation, similar to the standard approach for long-term calculations on a scatter diagram, as described in (NI 554: Design Sloshing Loads for LNG Membrane Tanks, 2011), Sect. 7.3 :

$$P_{LT}(X,T) = \left[\sum_{all\ config\ i} P_{short-term}(X|config_i).p_{config}(config_i) \right]^{\frac{T}{D_{config}}} \quad (9)$$

where:

- $P_{LT}(X,T)$ is the long-term non-exceedance probability, ie probability of not exceeding X in duration T,
- $P_{short-ter}\ (X|config_i)\ is$ short term non-exceedance probability, knowing the configuration, i.e. probability of not exceeding X in duration D_{config} on given sailing and loading conditions,
- p_{config} : Probability of the (loading condition, filling level, sailing conditions) configuration
- D_{config} : Stable configuration duration, typically taken equal to 3 hours.

The 25-year return level in terms of roll motion is defined as the value θ_{ART} so that $P_{LT}(\theta_{ART}, 25\ years) = 1/e$.

An analogous long-term calculation is carried out for the cases without ART in order to obtain θ_{NO-A} . A reduction factor can then be derived.

From an operational point of view, this "raw" reduction factor will be combined with a safety coefficient, describing the level of confidence in the calculation carried out, as well as in the relevance and accuracy of the inputs that have been considered (operational profile, roll damping coefficients, ART characterization, etc.).

III – ART responses - Validation of CFD - EGA as governing parameter

III – 1 ART geometry

The considered ART is figured out below:

Figure 2: ART geometry. Each solidity ratio is equal to 50% (ratio of the area of the baffle to the total area ART section) (3D view and section details).

This ART is equipped with three baffles located at one quarter, one half and three quarters of the tank's breadth. This configuration is classical for ARTs (Faltinsen & Timokha, 2009).The relative dimensions of the considered ART are the following ones: D/B=0.229, L/B=0.182 and H/B=0.102 where L, B, D and H denote respectively the ART's length, breadth, height and the filling level.

III – 2 Bench tests configuration

The ART is filled with water at ambient temperature. The considered liquid filling level is H/B=0.102. The complete experimental setup is described in (Lee S., 2015). This experimental set-up allows reproducing any forced roll motion around a horizontal axis. The ART (described in the previous sub-section) is fixed to the cradle. This experimental set-up is figured out below:

(a) Classical tests

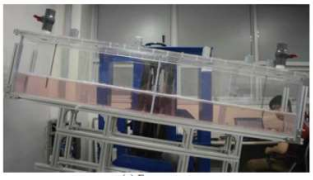

(b) Tests with a plate on the free surface of the ART ("double-body" bench tests).

Figure 3: Bench tests set-up with the ART (fixed to its cradle).

The time histories of exciting moment and oscillating angle are simultaneously measured from dynamometer and potentiometer, respectively. The measured exciting moment from the dynamometer contains also the effects such as the moment due to the mass of the cradle, tank (made of plexyglass®) etc… In order to compare experiments with CFD, one has to get rid of this "solid" component. To do so, one could perform bench tests with an empty tank. But, for these bench tests, it is decided to perform "double-body" tests with a plate located on the liquid free surface to restrain free surface deformations (equivalent to "double-body" flow).

The center of rotation is located at z/B (equal to 0.168) above the ART bottom. The tested forced roll motion angles are {3°, 6°, 9°} and thirteen periods are tested.

III – 3 Validation of CFD for ART responses

As mentioned above, in order to get rid of the "solid" component (mass of the cradle, tank etc…) of the ART torque measurement Mx(Exp), the final torque for the ART Mx(Exp) minus the torque for the "double body" configuration $M_x^{DB}(Exp)$ is considered for comparison with CFD. Thus, one can compare experiments and CFD in a relevant manner by considering the following quantities:

$$[M_x - M_x^{DB}]_{CFD} = M_x(CFD) - M_x^{DB}(CFD) \quad (9a)$$

$$[M_x - M_x^{DB}]_{Exp} = M_x(Exp) - M_x^{DB}(Exp) \quad (9b)$$

$$[M_x - M_x^{DB}]_{CFD} \text{ can be compared to } [M_x - M_x^{DB}]_{Exp} \text{ relevantly} \quad (9c)$$

$$[M_x - M_x^{DB}]_{CFD} = a(0)^{CFD} + \sum_{k=1}^{N} [a(k)^{CFD}\cos(k\omega t) + b(k)^{CFD}\sin(k\omega t)] \quad (9d)$$

$$[M_x - M_x^{DB}]_{Exp} = a(0)^{Exp} + \sum_{k=1}^{N} [a(k)^{Exp}\cos(k\omega t) + b(k)^{Exp}\sin(k\omega t)] \quad (9e)$$

$$\text{with } a(0) = 0, c(k) = \sqrt{a(k)^2 + b(k)^2}, c(tot) = \sqrt{\sum_{k=1}^{N} c(k)^2} \quad (9f)$$

This comparison between experiments and CFD is carried out for all tested roll forced motions amplitudes {3°, 6°, 9°} and periods.

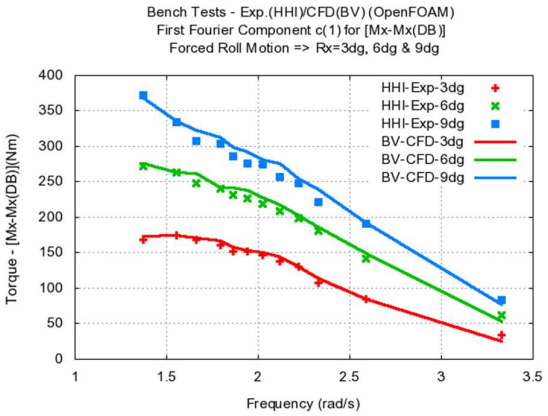

Figure 4: Comparison between experiments and CFD for $[M_x - M_x^{DB}]$ for c(1). Experimental results are depicted with points and CFD ones with lines.

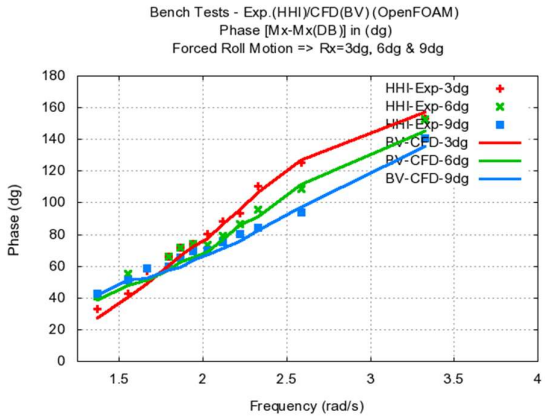

Figure 5: Comparison Exp./CFD for the phase shift between $[M_x - M_x^{DB}]$ and the forced roll motion.

First, one can notice the very good agreement between CFD and experimental results for both amplitude and phase. Then, one can notice that the ART response is non-linear (see amplitude and phase, Figure 4 and Figure 5): indeed if amplitude was linear then the amplitude for 9 degrees (blue curve) would equal to 3 times this one for 3 degrees (red curve) which is not the case obviously. This non-linear behavior is well captured by CFD. Also, the damping is significant as the phase (between Mx and the roll motion) is between 30° and 150° for a large range of periods.

As a conclusion, CFD is validated for the evaluation of a classical ART response.

III – 4 Validation of EGA as governing parameter

To demonstrate that the EGA is a governing parameter for the ART response, one considers the two following cases:

- Particular case mixing sway and roll motions such that EGA(t) is equal to 0 (at the ART's center of volume).
- General cases with two different motions (pure sway or pure roll) but having the same EGA at the center of volume of the ART ($\forall t$).

For these two cases, one compares the transverse force F_y and the roll moment M_x in the ship-fixed reference frame (inertial reference frame).

a) EGA(t)=0 at ART center of volume

One considers the particular case (mixing sway and roll) where EGA equals to zero (at any instant) at ART's center of volume. If the effective angle of gravity is a parameter that controls the response of antiroll tanks, then this specific case should be equivalent to the case of the tank at rest (for which the EGA is also equal to 0). The free surface is depicted in the figures below:

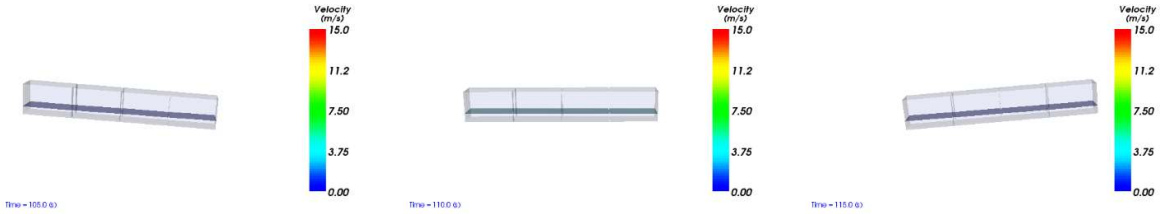

Figure 6: sway/roll combination such that $\forall t$, EGA(t)=0 at ART center of volume: sway(amp)=8.67m, roll(amp)=5.0dg; period=20.0s. The free surface elevation snapshots at t=110.0s, 115.0s and 120.0s are represented. As expected, the free surface remains flat.

As expected, the free surface remains flat which confirms that EGA seems to be a governing parameter for ARTs response.

b) Equivalence of pure sway & pure roll motions if EGA is same at ART center of volume

To demonstrate that the EGA is a governing parameter for the ART response, one compares two different motions (pure sway and pure roll) having the same EGA at the center of volume of the ART. One compares the transverse force F_y and the roll moment M_x in the ship-fixed reference frame (non-inertial reference frame).

For instance, the F_y and M_x time series are displayed hereafter for an EGA amplitude equal to 10° and a period equal to 19s for a pure sway and a pure roll motion.

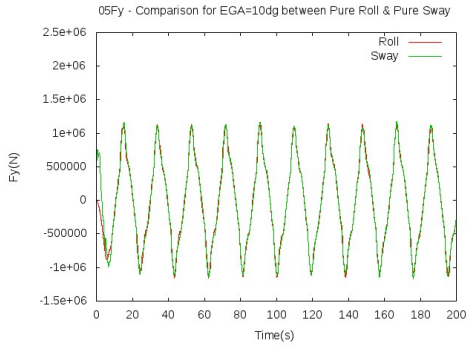

Figure 7a: Fy comparison between a pure sway and a pure roll motion having the same EGA amplitude equal to 10° (at ART center of volume) and same period T=19.0s.

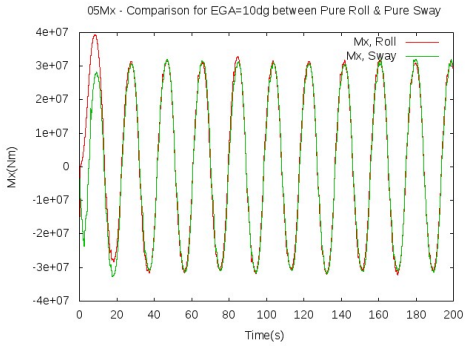

Figure 7b: Mx comparison between a pure sway and a pure roll motion having the same EGA amplitude equal to 10° (at ART center of volume) and same period T=19.0s.

The agreement for F_y, $M_x$time series between different motions having the same EGA is excellent.

In order to validate this equivalence between pure sway and pure roll motions (having the same EGA at the center of volume of the ART), we perform systematic CFD calculations (either sway or roll) for the following EGA amplitudes {1°, 2°, 5°, 10°, 15°, 20°} and periods {11s, 13s, 15s, 17s, 19s, 20.3s, 20.8s, 21.7s, 22.5s, 25s, 27s, 30s}. The comparison is carried out for roll moment amplitude.

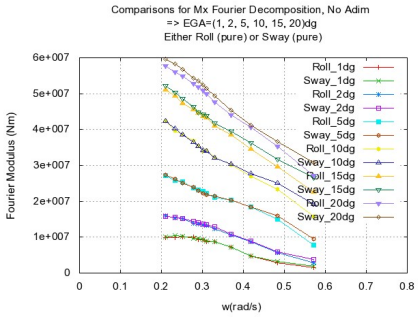

Figure 8a: Mx amp. comparison between pure sway & pure roll motions having the same EGA amplitude equal to{1°, 2°, 5°, 10°, 15°, 20°} and for 12 periods varying from 11s to 30s.

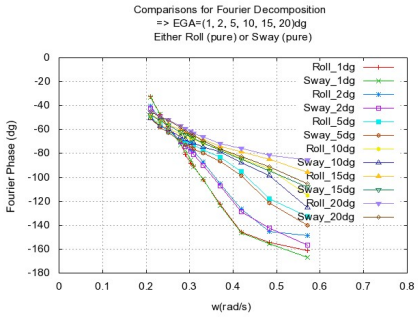

Figure 8b: Mx phase (relative to motion) comparison between pure sway and pure roll motions (same cases as in Figure 8a).

The agreement for M_x amplitudes and phases between different motions (pure sway or pure roll) having the same EGA is excellent. The same conclusion arises for the transverse force F_y.

IV – Application to seakeeping

The objective of this section is to compare the motions of a barge shaped ship equipped with ARTs measured during basin tests with those calculated by the methodology shown in II. The basin tests were carried out by HHI. To maximize the roll motion, beam sea case is considered (the wave heading is equal to 90°).

IV – 1 Basin tests

The following configuration (barge shaped ship + 3 ARTs) is considered:

(a) HHI basin tests (here without ARTs).

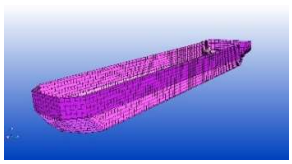

(b) Hydrodynamic mesh of the ship.

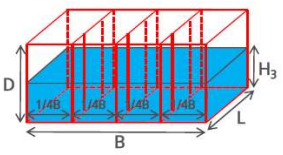

(c) ART configuration with 3 baffles located at one ¼, ½ and ¾ of tank's breadth.

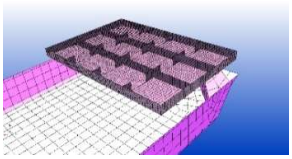

(d) Location and zoom on the hydrodynamic mesh of the ship and the 3 ARTs (aft part of the ship).

Fig. 9 Snapshots of the HHI basin tests, the barge-shaped ship and the three ARTs.

The ART size differs from this one considered in the first section. Dedicated CFD calculations were carried out for these new ARTs. However, as the configuration with 3 baffles is the same, ART response differs slightly. For sake of place, these results are not presented.

IV – 2 Potential calculations

For reference, pure potential calculations (HydroSTAR®) are carried out. For potential calculations, due attention is to be paid on the flat plates (here baffles). This is the reason why, two hydrodynamic meshes were considered for the ARTs: one with thin baffles and the other ones with thicker baffles as displayed on the figure below:

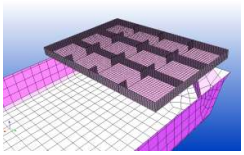

Figure 10a: Hydrodynamic mesh with thin baffles

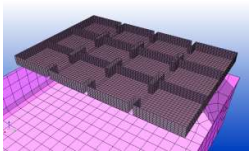

Figure 10b: Hydrodynamic mesh with thick baffles

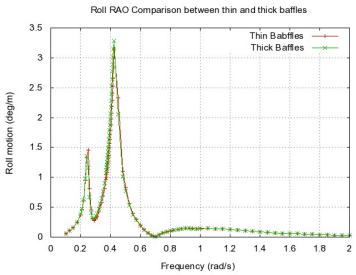

Figure 10c: Roll RAO comparison (pure potential) between hydrodynamic mesh with thin & thick baffles.

One can notice that the agreement between both hydrodynamic meshes for ARTs is very good. The small discrepancies are due to the fact that the hydrodynamic mesh with thick baffles reduces the ART mass and so the ART response. For the final potential calculations, the mesh with thin baffles is considered.

IV – 3 Experiments / Numerical calculations

The numerical roll transfer functions (obtained with different physical assumptions) are compared to the experimental one. In the following, the considered roll RAOs correspond to the following cases:

- numerical calculations (No ART): seakeeping calculations (for the ship only) using potential theory. Liquid within ARTs is considered as solid,
- numerical calculations (ART Stiff.): seakeeping calculations (for the ship only) using potential theory. Only the hydrostatic stiffness of ARTs is considered,
- numerical calculations (Potential): seakeeping calculations (for the ship only & the 3 ARTs) using potential theory. The liquid dynamic effects of the ARTs are taken into account using potential theory. The hydrodynamic mesh of these ARTs is displayed in Figure 10.
- numerical calculations (methodology section II): coupled seakeeping calculations potential-CFD using EGA (forced sway and roll motions are considered). Iteration procedure for EGA is applied,
- experiments with regular waves (Exp., A=1m, i.e. ±1m for free surface elevation)
- experiments with irregular waves (Exp., Hs=3.08m, Tp=17.32s). JONSWAP spectrum is considered with Hs=3.08m, Tp=17.32s and γ=3.3.

Comparison between these different numerical and experimental roll RAOs are displayed hereafter:

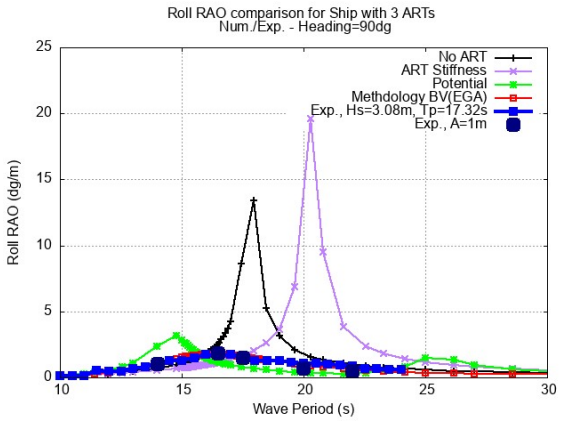

Figure 11a: Roll RAO comparison between experiments & numerical calculations for wave heading=90°.

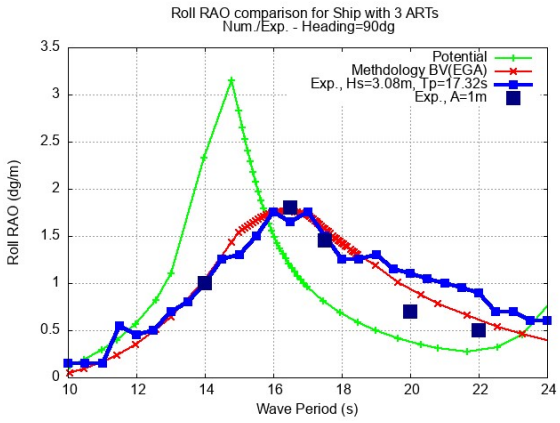

Figure 11b: Roll RAO comparison between experiments & numerical calculations for wave heading=90° (zoom of Figure 11a).

ARTs hydrostatic stiffness (No ART & ART Stiff.) do not agree at all with experimental roll RAO. The roll RAO using potential theory for both seakeeping and ARTs is closer to the experimental roll RAO but still some discrepancies can be noticed.

Finally, one can notice that agreement of BV methodology with the experimental roll RAO (regular and irregular waves) is very good.

V – Ship application

V – 1 Ship description

In 2019, the ship owner ordered a 15,000 TEU container ship equipped with an anti-roll tank to improve the crew's comfort, reduce fuel consumption, and enable the loading of heavier containers in a higher position than usual. Following the Bureau Veritas (BV) Rule NR 625, The ship owner requested BV to evaluate the roll reduction performance, as described in Section II.

V – 2 Assumptions for seakeeping calculations / operational profile

The following assumptions were made for the seakeeping calculations:

- Infinite water depth
- North Atlantic scatter diagram (Rec.34 Rev.1 2001)
- Short-crested waves (spreading with N=2)
- Roll radius of gyration ranging from 0.33*B to 0.42*B (depending on the loading conditions)
- GM versus draft (loading conditions) data was provided for container ships of similar capacities
- Speed profile was provided for container ships of similar capacities:
  - For Hs<9.0m $\Rightarrow V = V_d$ where V_d denotes design speed
  - For 9.0m ≤ Hs < 15.0m $\Rightarrow V = V_d/2$
  - For Hs ≥ 15.0m $\Rightarrow V = V_d/3$

V – 3 Comparison with full scale measurements for short-term sailing condition

To test the ART, some full-scale tests were carried out during a journey of the container ship:

- One hour (from 17h05 to 18h05) with ART filled (4m)
- One hour (from 18h15 to 19h15) with (nearly) empty tank

From GPS positions, it is possible to derive the ship's speed but also to retrieve metocean conditions encountered by the ship:

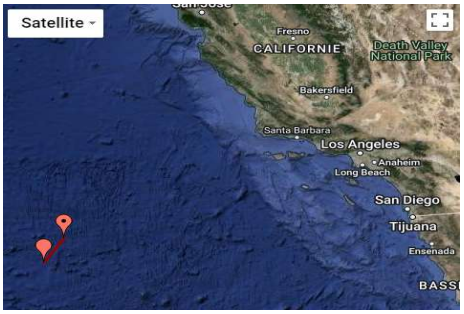

Figure 12a: GPS coordinates of the ship path during the ART test.

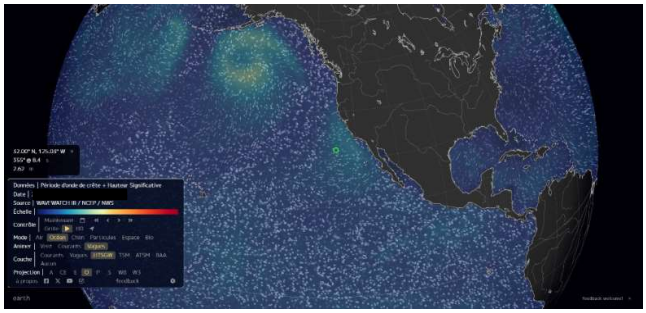

Figure 12b: Visualization of the waves during the full-scale tests (https://earth.nullschool.net/fr).

All the measurements and numerical calculations are presented below:

Return Of Experience (REX) - Measurements					Numerical calculations following BV methdology (CFD/potential-EGA)		
Speed	Wave height	Wave Heading		Roll RMS	Roll RMS - sqrt(m0)(dg)	Roll RMS - sqrt(m0)(dg)	Roll RMS - sqrt(m0)(dg)
Vrex(kn)	Hs(m)	β(deg)		sqrt(m0)(dg)	**Wave period - Tp=8.7s**	**Wave period - Tp=9.7s**	**Wave period - Tp=10.7s**
19.91	2.6	130	fART	43% roll reduction	37% croll reduction	38% roll reduction	40% reduction

Figure 13: Comparisons between measurements and numerical calculations. Sensitivity analysis on wave periods is carried out for the numerical calculations.

One can observe a very good agreement between the measurements and the numerical calculations.

V – 6 Roll reduction factors – long-term calculations

As the short-term sailing conditions are validated (previous section), one can carry out long-term calculations (25-year return period) taking into account the operational profile provided by the ship owner. Doing so and following procedure described in II - 9, the following roll reduction factors as function of GM can be obtained:

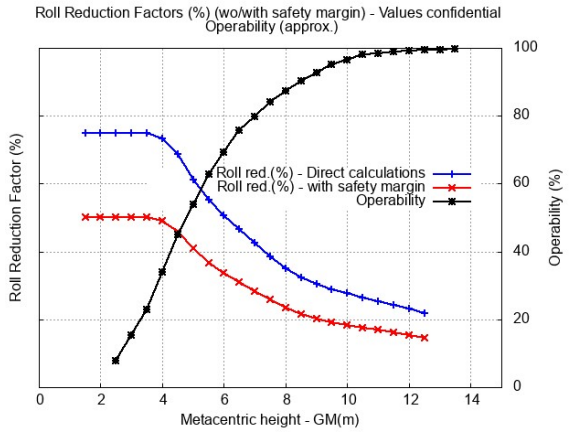

Figure 14: Final roll reduction factors (%) after long-term roll calculations (at 25-year return period) taking into account the ship's operational profile and the seakeeping assumptions (V-2).
The BV roll reduction factor can be obtained by f_{ART} = 1 – roll-reduction(%)/100

VI – Conclusions and discussion

A consistent methodology for considering anti-roll tanks in a potential seakeeping code was presented. To validate this methodology, different types of tests were presented: from forced motion tests to validate CFD calculations for the evaluation of ART response to basin model tests to validate the BV methodology (potential/CFD and EGA) for seakeeping applications. In addition, this methodology is also validated through some comparisons, which show excellent agreement, with full-scale measurements carried out on a container ship. Finally, the typical roll reduction coefficients for this type of container ship were presented.

In the future, additional validations using full-scale measurements will be carried out in order to decrease the safety margin that was considered in the beginning of the project due to lack of full-scale data.

References

Carette, N. (2015). A study of the response to sway motions of free surface anti-roll tanks. *Proceedings of the SNAME 5th World Maritime Technology Conference*.

Chen, X.-B. (2004). Hydrodynamics in Offshore and Naval Applications - Part I. *6th International Conference on Hydrodynamics.* Perth, Australia.

Faltinsen, O., & Timokha, A. (2009). *Sloshing.* Cambridge University Press.

Lee S., J. M.-K.-H.-B.-M. (2015). An Application of a Free Surface Type Anti-Rolling Tank on Ultra Large Container Ships. *15th ISOPE Conference.* Hawaii, USA.

Malenica Š., Z. M. (2003). Dynamic coupling of seakeeping and sloshing. Honolulu, USA.

(2011). *NI 554: Design Sloshing Loads for LNG Membrane Tanks.* Guidance Note, Bureau Veritas.

(2016). *NR 625 - Structural Rules for Container Ships.* Manual, Bureau Veritas.